

Two-time-scale Control of High-speed Permanent Magnet Synchronous Motors

Yan Zhang, Zhong Yang, Wenyong Duan, Xiaolin Wang, Xucong Bao

Abstract—A two-time-scale control strategy of high-speed permanent magnet synchronous motors (HSPMSMs) is proposed in this paper. HSPMSMs including mechanical part and electromagnetic part possess two-time-scale characteristic. Singular perturbation theory is adopted to model the two-time-scale dynamic behavior. The model is then decomposed into slow and fast subsystems. With the consideration of disturbances in both slow and fast subsystems, H_∞ controller and sliding mode controller are designed for slow and fast subsystems, respectively. Stabilities of the two subsystems are proven using Lyapunov theory separately. A composite controller is developed by combining the two subcontrollers, and the stability of the whole system is analyzed. Control performance of HSPMSM is verified through simulation experiments. Results show that the parallel-connection dual-loop two-time-scale control presents clear advantages over series-connection dual-loop PI control.

Index Terms—High-speed permanent magnet synchronous motors, two-time-scale control, H_∞ control, sliding mode control

I. INTRODUCTION

High-speed permanent magnet synchronous motors (HSPMSMs) are widely applied in national defense, aeronautics and astronautics, medical equipment, and other fields due to their microminiature, light weights, high efficiency, and high power density [1]. Hence HSPMSMs have attracted considerable research attention from industrial and academic communities [2], [3]. As known to all, control strategy plays a very important role in improving the working performance of motors. PID control [4], dead-beat control [5], model predictive control [6], adaptive control [7], [8], etc. are commonly applied to control electric current loop and angular velocity loop of HSPMSMs. However, these control methods

Manuscript received May 10, 2022; revised November 29, 2022. This work was jointly supported by the Natural Science Foundation of the Jiangsu Higher Education Institutions of China under Grant 21KJB120003, National Natural Science Foundation of China under Grant 52177048, Natural Science Foundation of Jiangsu Province under Grant BK20201297, and Industry university research cooperation project of Jiangsu Province under Grant BY2021358.

Y. Zhang is a lecturer of College of Intelligent Science and Control Engineering, Jinling Institute of Technology, Jiangning District, Nanjing 211169; she is also working as a postdoctor in College of Automation Engineering, Nanjing University of Aeronautics and Astronautics, Jiangning District, Nanjing 211106, China. (corresponding author, phone: 86-025-86188535, e-mail: iamzhangyan123@126.com)

Z. Yang is a professor of College of Intelligent Science and Control Engineering, Jinling Institute of Technology, Jiangning District, Nanjing 211169, China. (e-mail: yz@jit.edu.cn)

W. Duan is an associate professor of College of Electrical Engineering, Yancheng Institute of Technology, Tinghu District, Yancheng 224051, China. (e-mail: dwy1985@126.com)

X. Wang is a professor of College of Automation Engineering, Nanjing University of Aeronautics and Astronautics, Jiangning District, Nanjing 211106, China. (e-mail: wangxl@nuaa.edu.cn)

X. Bao is a Ph.D candidate in the College of Automation Engineering, Nanjing University of Aeronautics and Astronautics, Jiangning District, Nanjing 211106, China. (e-mail: baexc@nuaa.edu.cn)

are typically based on series-connection dual-loop structure as shown in Fig. 1.

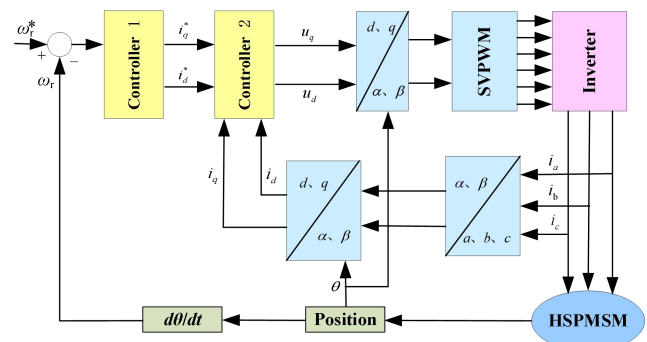


Fig. 1. Series-connection Dual-loop Control Strategy.

In the series-connection dual-loop control strategy, current loop is regarded as inner loop, and angular velocity loop (or position loop) is taken as outer loop. The currents references are provided by the outer loop controller and angular velocity (or position) tracking error. The design processes of controllers for inner and outer loops are affected by each other. Notably, poor control performance of the outer loop will lead to an unsatisfactory reference of the q axis current and poor inner loop control results. Therefore, developing two acceptable controllers at the same time and obtaining excellent performance of the entire system are usually complex and difficult.

HSPMSMs include mechanical and electromagnetic parts. In the system, current dynamics are remarkably faster than mechanical dynamics [9], [10]. Hence, HSPMSMs demonstrate two-time-scale property. Two-time-scale system is a typical simplified representative of multi-time-scale systems. In this paper, a novel parallel-connection dual-loop control strategy is proposed for HSPMSMs based on the two-time-scale characteristic and singular perturbation theory.

Singular perturbation theory is an effective tool to deal with two-time-scale systems [11], [12]. The two-time-scale system is decoupled into slow and fast subsystems, and two subcontrollers are designed separately on the basis of these two subsystems. A composite controller can then be developed by combining the two subcontrollers, as shown in Fig. 2. This method presents many advantages and is applicable to plenty of electromechanical integrated systems with two-time-scale property [13], [14].

Reference [15] presents an application of singular perturbation theory for modeling induction motors systems and shows that singular perturbation techniques can provide an effective means to represent the dynamics of motor states. However, control problem is ignored in [15]. Singular perturbation theory is utilized in [16], [17] to establish a

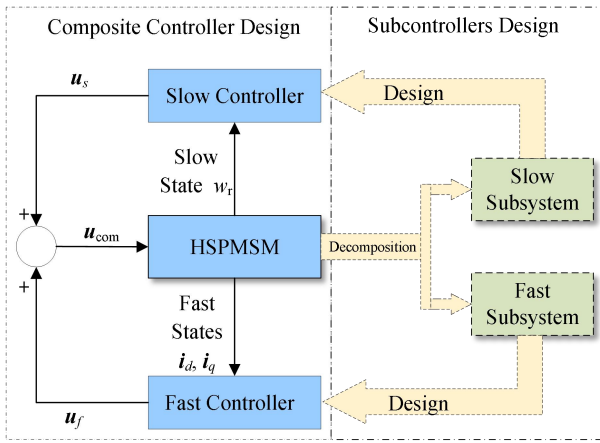


Fig. 2. Singular Perturbation Control Strategy.

torque control method for permanent magnet stepper motors. Although the slow subcontroller is designed, the fast subsystem is neglected. Reference [18] develops a two-time-scale observer for induction machines and demonstrates the convergence of the observer for all open-loop stable operating points of the induction machine. To our best knowledge, the composite two-time-scale control scheme for HSPMSMs remains unverified.

Singular perturbation theory is applied in this work to develop a parallel-connection dual-loop control strategy for HSPMSMs, and the block diagram of the proposed method is shown in Fig. 3. First, the HSPMSM model is rearranged into singular perturbation form, and two decomposed subsystems are obtained via mathematical derivations. Second, fast and slow subcontrollers are designed for fast and slow subsystems, respectively. Finally, a composite controller is developed on the basis of the two subcontrollers for HSPMSMs.

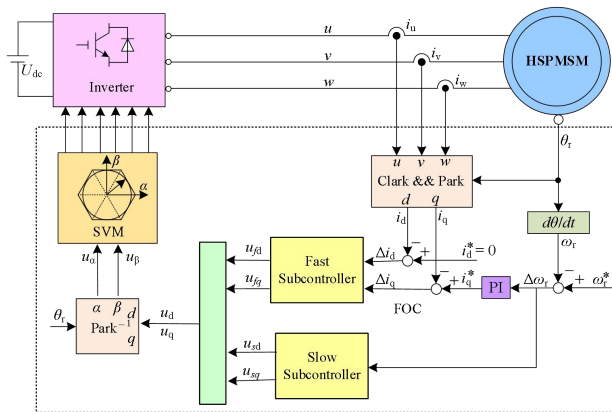


Fig. 3. Parallel-connection Dual-loop Control Strategy.

The main contributions of this study are presented as follows: (1) a parallel-connection dual-loop control strategy for HSPMSMs is proposed; (2) an H_{∞} controller is designed using the linear parameter varying reformulation for the slow subsystem and a sliding mode controller for the fast subsystem while considering disturbances in both subsystems. The affections of subcontrollers from each other are avoided given that the two-time-scale controllers are designed separately. The control design process is simplified and the computational burden is reduced. The performance of the HSPMSM under two-time-scale control and PI control

are compared via simulations, and advantages of the method proposed in this paper are validated.

II. SYSTEM MODEL OF HSPMSMs

In this section the HSPMSMs model is presented. Slow and fast subsystems are then derived to provide the basis of the subcontrollers design.

The following model considers a class of HSPMSMs:

$$L_d \dot{i}_d(t) = u_d(t) - r i_d(t) + \omega_e(t) L_q i_q(t) \quad (1)$$

$$L_q \dot{i}_q(t) = u_q(t) - r i_q(t) - \omega_e(t) (L_d i_d(t) + \Psi_f) \quad (2)$$

$$J \dot{\omega}_e(t) = P_n (\Psi_f i_q(t) + (L_d - L_q) i_d(t) i_q(t) - T_l) - B \omega_e(t) \quad (3)$$

where $i_d(t)$ and $i_q(t)$ are the direct and quadrature axis currents respectively, L_d and L_q are the direct and quadrature axis inductances respectively, $u_d(t)$ and $u_q(t)$ are the direct and quadrature axis voltages respectively, r is the stator resistance, $\omega_e(t)$ is the electrical angular velocity, Ψ_f is the magnet flux linkage, J is the rotor inertia, P_n is the number of pole pairs, T_l is the load torque which is assumed to be a constant, and B is the damping coefficient.

For non-salient pole motors $L_d = L_q$, so equation (3) is simplified to be

$$J \dot{\omega}_e(t) = P_n \Psi_f i_q(t) - P_n T_l - B \omega_e(t) \quad (4)$$

The complete nonlinear model of HSPMSM is obtained by combining (1), (2) and (4). We will then introduce the singular perturbation method to decouple currents and angular velocity variables.

The order of magnitude of inductances in HSPMSM is usually 10^{-3} or even smaller. Hence, absolute values of $i_d(t)$, $i_q(t)$ are considerably larger than that of $\dot{\omega}_e(t)$. This finding implies that variation rates of $i_d(t)$ and $i_q(t)$ are faster than that of $\dot{\omega}_e(t)$. This conjecture coincides with the common sense that the electrical part of the system changes remarkably faster than the mechanical part. Therefore, we take $i_d(t)$, $i_q(t)$ as fast variables and $\dot{\omega}_e(t)$ as the slow variable. The singular perturbation parameter is defined as $\epsilon = 1 \times 10^{-3}$ in view of the order of magnitude of inductances to obtain the following:

$$\epsilon \dot{i}_d(t) = \frac{u_d(t)}{\bar{L}} - \frac{r i_d(t)}{\bar{L}} + \frac{\omega_e(t) L i_q(t)}{\bar{L}} \quad (5)$$

$$\epsilon \dot{i}_q(t) = \frac{u_q(t)}{\bar{L}} - \frac{r i_q(t)}{\bar{L}} - \frac{\omega_e(t) (L i_d(t) + \Psi_f)}{\bar{L}} \quad (6)$$

$$\dot{\omega}_e(t) = \frac{P_n}{J} \Psi_f i_q(t) - \frac{P_n}{J} T_l - \frac{B \omega_e(t)}{J} \quad (7)$$

where $\bar{L} = L \times 10^3$ and $L \triangleq L_d = L_q$.

The obtained nonlinear singularly perturbed model of HSPMSMs is then applied to decouple the fast and slow states of system (5)-(7) using singular perturbation theory.

Set $\epsilon = 0$ in (5) and (6) to obtain the two formulas (8)-(9) of $i_{ds}(t)$ and $i_{qs}(t)$ to describe the slow portions of the respective fast states $i_d(t)$ and $i_q(t)$.

$$i_{ds}(t) = \frac{\omega_{es}(t) L}{r} + \frac{u_{ds}(t)}{r} \quad (8)$$

$$i_{qs}(t) = -\frac{\omega_{es}(t) L^2}{r^2} - \frac{\omega_{es}(t) \Psi_f}{r} - \frac{\omega_{es}(t) L}{r^2} u_{ds}(t) + \frac{u_{qs}(t)}{r} \quad (9)$$

where the subscript s signifies the slow parts of variables.

We can obtain the following equation when substituting (8) and (9) into (7):

$$\begin{aligned}\dot{\omega}_{es}(t) &= \frac{P_n}{J}\Psi_f \left(-\frac{\omega_{es}^2(t)L^2}{r^2} - \frac{\omega_{es}(t)\Psi_f}{r} \right. \\ &\quad \left. - \frac{\omega_{es}(t)L}{r^2}u_{ds}(t) + \frac{u_{qs}(t)}{r} \right) - \frac{T_l P_n}{J} - \frac{B\omega_e(t)}{J} \\ &= -\frac{P_n L^2}{J r^2} \Psi_f \omega_{es}^2(t) - \left(\frac{P_n}{J r} \Psi_f^2 + \frac{B}{J} \right) \omega_{es}(t) \quad (10) \\ &\quad + \left[-\frac{P_n L}{J r^2} \Psi_f \omega_{es}(t) \quad \frac{P_n}{J r} \Psi_f \right] \begin{bmatrix} u_{ds}(t) \\ u_{qs}(t) \end{bmatrix} - \frac{T_l P_n}{J}\end{aligned}$$

Remark 2.1: ϵ is a very small positive parameter. We can obtain the approximation relations (8)-(9) between the fast states $i_d(t)$, $i_q(t)$ and the slow state $\omega_e(t)$ by setting $\epsilon = 0$ so as to decouple the fast and slow states in (5)-(7). However, (8)-(9) only reveal the approximate equations of slow sections of the actual fast and slow states by ignoring the tiny parameter ϵ . This indicates that small errors exist between (8)-(9) and the original model (5)-(7). Therefore, we will further derive fast portions of actual fast and slow states to compensate for the errors caused by neglect of ϵ during decoupling.

The following notations are used to simplify (10): $a_1 = -\frac{P_n L^2}{J r^2} \Psi_f$, $a_2 = -\frac{P_n}{J r} \Psi_f^2 - \frac{B}{J}$, and $b = \left[-\frac{P_n L}{J r^2} \Psi_f \omega_{es}(t) \quad \frac{P_n}{J r} \Psi_f \right]$. Equation (10) is then transformed as follows:

$$\begin{aligned}\dot{\omega}_e(t) &= a_1 \omega_{es}^2(t) + a_2 \omega_{es}(t) + b(\omega_{es}) \begin{bmatrix} u_{ds}(t) \\ u_{qs}(t) \end{bmatrix} - \frac{T_l P_n}{J} \\ &= (a_1 \omega_{es}(t) + a_2) \omega_{es}(t) + b(\omega_{es}) \begin{bmatrix} u_{ds}(t) \\ u_{qs}(t) \end{bmatrix} - \frac{T_l P_n}{J} \quad (11)\end{aligned}$$

System (11) is the slow subsystem which describes the main dynamic behavior of the slow variable of the system. It can be seen from (11) that the slow subsystem is a nonlinear model.

The fast subsystem is derived as follows. Define $\tau = \frac{t-t_0}{\epsilon}$ and change the time scale of (5)-(6) from t to τ , we obtain

$$\frac{di_{df}}{d\tau} = -r i_{df} + \bar{\omega}_e L + u_{df} + d(\tau) \quad (12)$$

$$\frac{di_{qf}}{d\tau} = -\bar{\omega}_e L i_{df} - r i_{qf} + u_{qf} - \bar{\omega}_e \Psi_f + d(\tau) \quad (13)$$

In view of the fast time scale τ , ω_e is regarded as a constant denoted as $\bar{\omega}_e$ within a short time because of its slow variation feature. $u_d^p = \bar{\omega}_e L + u_{df}$ and $u_q^p = u_{qf} - \bar{\omega}_e \Psi_f$ are taken as pseudo inputs, and $d(t)$ is the disturbance bounded with $\|d(t)\|_2 < \delta$, $\delta > 0$.

Equations (12) and (13) can be rewritten as

$$\underbrace{\begin{bmatrix} \frac{di_{df}}{d\tau} \\ \frac{di_{qf}}{d\tau} \end{bmatrix}}_{\frac{dz}{d\tau}} = \underbrace{\begin{bmatrix} -r & 0 \\ -\bar{\omega}_e L & -r \end{bmatrix}}_{A_f} \underbrace{\begin{bmatrix} i_{df} \\ i_{qf} \end{bmatrix}}_z + \underbrace{\begin{bmatrix} u_d^p(\tau) \\ u_q^p(\tau) \end{bmatrix}}_{u_f} + \begin{bmatrix} 1 \\ 1 \end{bmatrix} d(\tau) \quad (14)$$

namely,

$$\frac{dz(\tau)}{d\tau} = A_f z(\tau) + u_f(\tau) + \begin{bmatrix} 1 \\ 1 \end{bmatrix} d(\tau) \quad (15)$$

The fast subsystem (15) is clearly a linear system.

Remark 2.2: The original system composed of (1), (2) and (4) is decomposed into slow subsystem (11) and fast

subsystem (15), and the slow mechanical state and fast electromagnetic states are decoupled. In the next section the designs of slow and fast subcontrollers are considered separately to simplify the synthesis complexity and difficulty.

III. MAIN RESULTS

The main results of this study, slow controller design method for the slow subsystem (11) and fast controller design method for the fast subsystem (15), are presented in the form of two theorems.

A. Slow Controller

The design of a gain-scheduled H_∞ controller is framed in the context of linear parameter varying (LPV) slow systems to regulate the electrical angular velocity with the consideration of nonlinearity and disturbance.

Choose an operating point $\theta_1 = \hat{\omega}_{es}$ of system (11) and linearize the nonlinear parts at point θ_1 to obtain the following:

$$\begin{aligned}\delta \dot{\omega}_{es} &= \dot{\omega}_{es} - \dot{\hat{\omega}}_{es} \\ &= (2a_1 \hat{\omega}_{es} + a_2) \delta \omega_{es} \\ &\quad + \begin{bmatrix} -\frac{P_n L}{J r^2} \Psi_f \delta \omega_{es}(t) & 0 \end{bmatrix} \begin{bmatrix} \hat{u}_{ds} \\ \hat{u}_{qs} \end{bmatrix} \\ &\quad + \begin{bmatrix} -\frac{P_n L}{J r^2} \Psi_f \hat{\omega}_{es}(t) & \frac{P_n}{J r} \Psi_f \end{bmatrix} \begin{bmatrix} \delta u_{ds}(t) \\ \delta u_{qs}(t) \end{bmatrix} \quad (16)\end{aligned}$$

A pseudo input is defined as follows:

$$\begin{aligned}u_s(\theta_1) &= \begin{bmatrix} -\frac{P_n L}{J r^2} \Psi_f \delta \omega_{es}(t) & 0 \end{bmatrix} \begin{bmatrix} \hat{u}_{ds} \\ \hat{u}_{qs} \end{bmatrix} \\ &\quad + \begin{bmatrix} -\frac{P_n L}{J r^2} \Psi_f \hat{\omega}_{es}(t) & \frac{P_n}{J r} \Psi_f \end{bmatrix} \begin{bmatrix} \delta u_{ds}(t) \\ \delta u_{qs}(t) \end{bmatrix} \quad (17)\end{aligned}$$

Equation (16) is then transformed as below:

$$\delta \dot{\omega}_{es} = (2a_1 \hat{\omega}_{es} + a_2) \delta \omega_{es} + u_s(\theta_1) \quad (18)$$

The nonlinear decoupled slow subsystem is linearized at one operating point θ_1 , and we can design a robust H_∞ controller on the basis of linear time invariant system (18). Take the disturbance and the output variable into consideration, and denote $A_s(\theta_1) \triangleq 2a_1 \hat{\omega}_{es} + a_2$ to obtain the following linearized system:

$$\delta \dot{\omega}_{es} = A_s(\theta_1) \delta \omega_{es} + u_s(\theta_1) + c \delta v \quad (19)$$

$$y = m \delta \omega_{es} \quad (20)$$

where δv is the external disturbance and m is a coefficient. The output is basically $\delta \omega_{es}$ in the case of $m = 1$.

We design the state feedback control input as follows:

$$u_s(\theta_1) = K(\theta_1) \delta \omega_{es} \quad (21)$$

We can obtain the following equation when $u_s(\theta_1)$ is substituted into (19)-(20):

$$\delta \dot{\omega}_{es} = (A_s(\theta_1) + K(\theta_1)) \delta \omega_{es} + c \delta v \quad (22)$$

The main result to guarantee the asymptotic stability of the system (22) is presented in Theorem 3.1.

Theorem 3.1: For system (22), given a positive scalar $\gamma > 0$, if there exists a positive parameter $P_1 > 0$ satisfying the following condition:

$$\begin{bmatrix} 2(A_s(\theta_1) + K(\theta_1))P_1 & cP_1 & d \\ cP & -\gamma^2 & 0 \\ d & 0 & -I \end{bmatrix} < 0 \quad (23)$$

then the equilibrium point of system (22) at θ_1 point is asymptotically stable, and the transfer function $T_{\delta v y}(s)$ from disturbance δv to output $y(t)$ satisfies $\|m(sI - (2a_1\hat{\omega}_{es} + a_2))^{-1}c\| < \gamma$.

The proof is simple and omitted here. The derivation details are referred to [20].

The domain of angular velocity, denoted by Ω , can be covered by appropriately choosing n operating points θ_i ($i = 1, \dots, n$) with $\theta_1 < \theta_2 < \dots < \theta_n$. In other words, θ_i , $i \in \{1, \dots, n\}$ constantly exists for any $\omega_{es} \in \Omega$, such that

$$\theta_i < \omega_{es} < \theta_{i+1} \text{ or } \omega_{es} = \theta_i \quad (24)$$

We can have n linear models by linearization of (11) at θ_i , $i \in \{1, \dots, n\}$. Then we design n controllers of these models at n operating points using Theorem 3.1 respectively. If $\omega_{es} = \theta_i$, then the control gain $K(\theta_i)$ is selected. Else, it is necessary to calculate two scalars $\alpha_1 > 0$ and $\alpha_2 > 0$ to satisfy $\omega_{es} = \alpha_1\theta_i + \alpha_2\theta_{i+1}$ and $\alpha_1 + \alpha_2 = 1$. The control gain is then selected as

$$K(t) = \alpha_1 K(\theta_i) + \alpha_2 K(\theta_{i+1}) \quad (25)$$

Remark 3.1: The interval Ω is cut into $n-1$ small sections by appropriately choosing n operating points θ_i satisfying (24). Only one case: (1) $\omega_{es} = \theta_i$ or (2) $\omega_{es} = \alpha_1\theta_i + \alpha_2\theta_{i+1}$ with $\alpha_1 > 0$ and $\alpha_2 > 0$ exists according to basic linear algebra theory. Case (1) is equal to $\omega_{es} = 1 \times \theta_i + 0 \times \theta_{i+1}$, where $\alpha_1 = 1$, $\alpha_2 = 0$. Therefore, α_1 and α_2 will always exist for any $\omega_{es} \in \Omega$ such that $0 \leq \alpha_1 \leq 1$, $0 \leq \alpha_2 \leq 1$ and $\omega_{es} = \alpha_1\theta_i + \alpha_2\theta_{i+1}$.

Remark 3.2: This control algorithm is based on the gain scheduling control method [21], [22]. The proof is excluded from this work because the asymptotic stability of the whole system under control (25) can be easily proven.

The following algorithm is presented to clarify the whole process of designing a parameter dependent controller for the nonlinear slow subsystem (11):

Algorithm of designing a parameter dependent controller

1. Choose n operating points θ_i ($i = 1, \dots, n$) with $\theta_1 < \dots < \theta_n$, such that the range of the rotor speed Ω can be covered;
2. Linearize the nonlinear singularly perturbed model (11) at θ_i , and obtain the linear parameter dependent coefficient $A_s(\theta_i)$;
3. For a given $\gamma > 0$, LMI (23) is solved at each operating point θ_i ($i = 1, \dots, n$) to obtain control gain matrices $K(\theta_i)$;
4. Measure the variable $\omega_{es}(t_k)$ at time t_k , and calculate weighting coefficients α_1 and α_2 to satisfy $\omega_{es} = \alpha_1\theta_i + \alpha_2\theta_{i+1}$ with $\alpha_1 \geq 0$, $\alpha_2 \geq 0$ and $\alpha_1 + \alpha_2 = 1$;
5. Obtain the control gain at time t_k :

$$K(t_k) = \alpha_1 K(\theta_i) + \alpha_2 K(\theta_{i+1})$$
 with the control input as follows:

$$u_s(t_k) = K(t_k)\delta\omega_{es}(t)$$
6. Apply the control input $u_s(t_k)$ to the slow subsystem (11);
7. At time t_{k+1} repeat step 4 to step 7.

B. Fast Controller

Considering the fast time scale of subsystem (14), sliding mode control method is chosen to guarantee fast dynamic response property for the fast subsystem (14) in this study.

We can obtain a reference trajectory of the states of fast subsystem with $z^{ref}(\tau) = [i_d^{ref}(\tau) \ i_q^{ref}(\tau)]^T$ by means of PI compensation in Fig. 3. The tracking error vector can be expressed as follows:

$$e(\tau) = \begin{bmatrix} i_d(\tau) \\ i_q(\tau) \end{bmatrix} - \begin{bmatrix} i_d^{ref}(\tau) \\ i_q^{ref}(\tau) \end{bmatrix} \quad (26)$$

We define a set of surfaces denoted by S as follows:

$$S = \left\{ e(\tau) \mid s(e(\tau)) = e(\tau) + M \int_0^\tau e(\theta) d\theta \right\} \quad (27)$$

where M is a given diagonal matrix satisfying $M = \text{diag}\{\lambda_1, \lambda_2\} > 0$, where $\lambda_i > 0$, $i = 1, 2$. The solutions of $s(\tau) = 0$ are $e_i(\tau) = e_i(0)e^{-\lambda_i\tau}$, $i = 1, 2$, where $e_i(\tau)$ is the i th element of vector $e(\tau)$, and $e_i(0)$ is the initial value of $e(\tau)$. The desired tracking dynamics of i_d, i_q in the sliding mode surfaces can be achieved with an appropriate selection of M .

Theorem 3.2: For given scalars $h > 0$, $l > 0$, and the upper bound of disturbances $\zeta > 0$, the closed-loop fast subsystem composed of (14) and (15) is considered with the following sliding mode control law:

$$u_f(\tau) = u_{eq}^n(\tau) - Qs(\tau) - P_2 \frac{s(\tau)}{\|s(\tau)\|_2 + h} \quad (28)$$

where Q and P_2 are positive definite matrices, and

$$u_{eq}^n(\tau) = - \left(A_f \begin{bmatrix} i_d^f(\tau) \\ i_q^f(\tau) \end{bmatrix} - \begin{bmatrix} i_d^{ref}(\tau) \\ i_q^{ref}(\tau) \end{bmatrix} + M \begin{bmatrix} i_d^f(\tau) \\ i_q^f(\tau) \end{bmatrix} - M \begin{bmatrix} i_d^{ref}(\tau) \\ i_q^{ref}(\tau) \end{bmatrix} \right) \quad (29)$$

Tracking errors of the closed-loop fast subsystem converge to zero if gains and parameters of the controller satisfy

$$P_2 > 0, \quad Q > 0 \quad (30)$$

$$\lambda_{\min}(Q)\|s(\tau)\|_2^2 + \lambda_{\min}(P_2)\|s(\tau)\|_2^2 > l + \|s(\tau)\|_2\zeta \quad (31)$$

Proof: Construct the following quadratic Lyapunov function:

$$V(\tau) = \frac{1}{2} s^T(\tau) s(\tau) \quad (32)$$

Take the derivative of $V(\tau)$ with respect to time τ to yield

$$\dot{V}(\tau) = s^T(\tau)\dot{s}(\tau) = V_{eq}(\tau) + V_N(\tau) \quad (33)$$

where $V_{eq}(\tau) = -s^T(\tau)Qs(\tau)$ and $V_N(\tau) = -s^T(\tau)P_2 \text{sgn}(s(\tau))$, with P_2 and Q satisfying

$$\begin{aligned} \dot{s}(\tau) + Qs(\tau) + P_2 \text{sgn}(s(\tau)) &= 0 \\ \text{or } s^T(\tau)(\dot{s}(\tau) + Qs(\tau) + P_2 \text{sgn}(s(\tau))) &= 0 \end{aligned} \quad (34)$$

The derivative of $s(\tau)$ can be expressed as

$$\begin{aligned} \dot{s}(\tau) &= \frac{\partial s}{\partial \tau} + \frac{\partial s}{\partial z} \frac{\partial z}{\partial \tau} \\ &= \frac{dz(\tau)}{d\tau} - \frac{dz^{ref}(\tau)}{d\tau} + Mz(\tau) - Mz^{ref}(\tau) \\ &= A_f z(\tau) + u_f + \begin{bmatrix} 1 \\ 1 \end{bmatrix} d(\tau) - \frac{dz^{ref}(\tau)}{d\tau} \\ &\quad + Mz(\tau) - Mz^{ref}(\tau) \end{aligned} \quad (35)$$

We can obtain the following equation by substituting (35) into (34):

$$u_f(\tau) = -\left(A_f z(\tau) + \begin{bmatrix} 1 \\ 1 \end{bmatrix} d(\tau) - \frac{dz^{ref}(\tau)}{d\tau} + Mz(\tau) - Mz^{ref}(\tau)\right) - Qs(\tau) - P_2 \text{sgn}(s(\tau)) \quad (36)$$

Denote $u_{eq}(\tau) = -\left(A_f z(\tau) + \begin{bmatrix} 1 \\ 1 \end{bmatrix} d(\tau) - \frac{dz^{ref}(\tau)}{d\tau} + Mz(\tau) - Mz^{ref}(\tau)\right) = u_{eq}^n(\tau) + u_{eq}^d(\tau)$, where $u_{eq}^n(\tau) = -\left(A_f z(\tau) - \frac{dz^{ref}(\tau)}{d\tau} + Mz(\tau) - Mz^{ref}(\tau)\right)$ is the nominal part and $u_{eq}^d(\tau) = -\begin{bmatrix} 1 \\ 1 \end{bmatrix} d(\tau)$ is the uncertain part.

On the basis of the assumption $\|d(\tau)\|_2 < \zeta$, we can ignore the uncertain part $u_{eq}^d(\tau)$ in $u_{eq}(\tau)$ to simplify the fast control law to yield

$$u_f(\tau) = u_{eq}^n(\tau) - Qs(\tau) - P_2 \text{sgn}(s(\tau)) \quad (37)$$

The following inequation is necessary to satisfy the reaching condition within a finite time:

$$\dot{V}(\tau) = s^T(\tau)\dot{s}(\tau) < -l \quad (38)$$

where l is a given small positive scalar. Then the following inequation can be derived by substituting (35) and (37) into (38):

$$\begin{aligned} & s^T(\tau)\dot{s}(\tau) \\ &= s^T(\tau) \left(\begin{bmatrix} 1 \\ 1 \end{bmatrix} d(\tau) - Qs(\tau) - P_2 \text{sgn}(s(\tau)) \right) \\ &< -l \end{aligned} \quad (39)$$

According to Schwarz inequality, (31) is a sufficient condition for (39). The following approximation is used in (31) to avoid discontinuity of control signals:

$$\text{sgn}(s(\tau)) = \frac{s(\tau)}{|s(\tau)| + h}$$

The fast subcontroller $u_f(\tau)$ can be obtained on the basis of Theorem 3.2.

Remark 3.3: References [16], [17] study the stability of fast subsystem and find that the fast subsystem without disturbances $d(t)$ is inherently exponentially stable. However, disturbances must be considered because they inevitably exist in practice. Therefore, a fast controller for the disturbed fast subsystem based on the sliding mode control method is designed in this study.

IV. NUMERICAL EXPERIMENTS

One numerical example is adopted in this section to verify the theoretical results. The simulation test is carried out using a 200 W motor. The main parameters of the motor are listed in Table I. The series-connection dual-loop PI control method is compared with the parallel-connection dual-loop two-time-scale control method. The fast control inputs obtained using the two-time-scale control scheme are presented in Fig. 4, and slow control inputs, u_{sd} , u_{sq} are presented in Fig. 5.

The control results of PI control are illustrated in Fig. 6, and two-time-scale control in Fig. 7. Fig. 6 and 7 show that the control results are both acceptable under these two

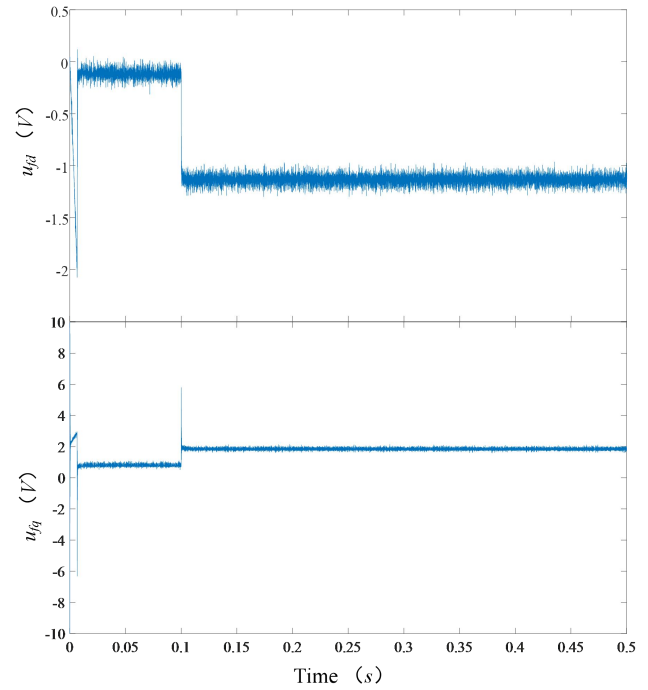


Fig. 4. Fast Portions of u_d and u_q : (a) Fast Portion of u_d , (b) Fast Portion of u_q .

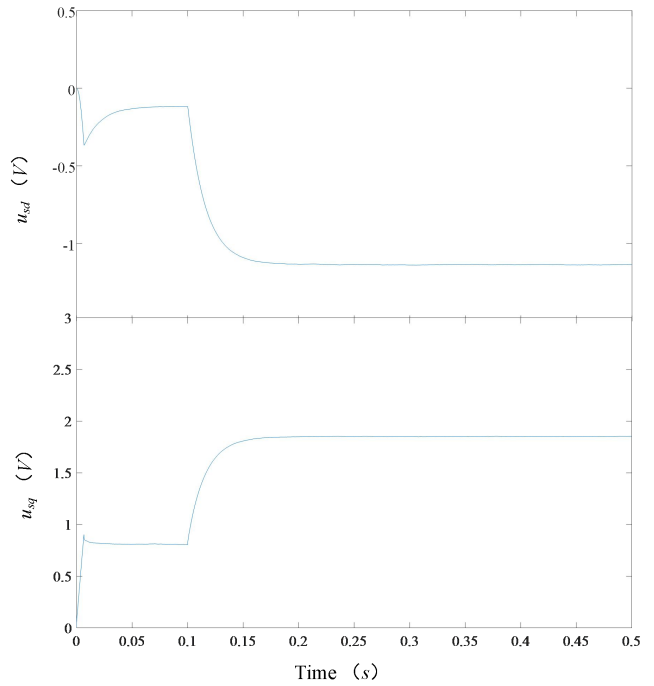


Fig. 5. Slow Portions of u_d and u_q : (a) Slow Portion of u_d , (b) Slow Portion of u_q .

TABLE I
MOTOR PARAMETERS

Descriptions	Values
Equivalent resistance	0.22 Ω
Equivalent inductance	0.0001 H
Stator flux amplitude	0.0004
Rated velocity	180,000 rpm
Number of pole pairs	1
Bus voltage	36 V
Rotor inertia	0.2 $\text{K}\cdot\text{m}^2$

control schemes although the performance of the two-time-

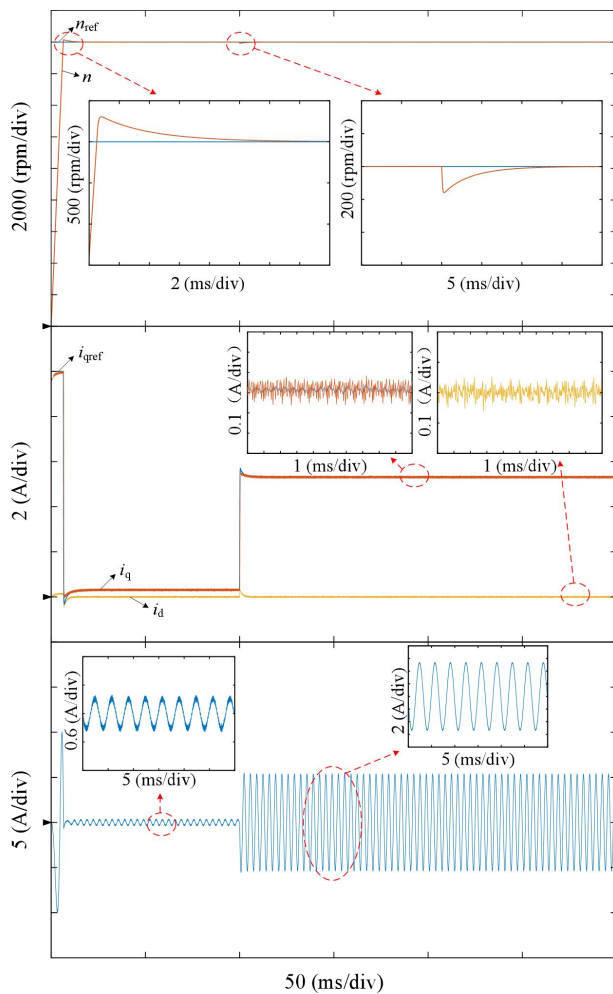


Fig. 6. Simulation Results under Series-connection Dual-loop PI Control: (a) Speed Dynamic, (b) Currents Performance, (c) Phase Current Waveforms.

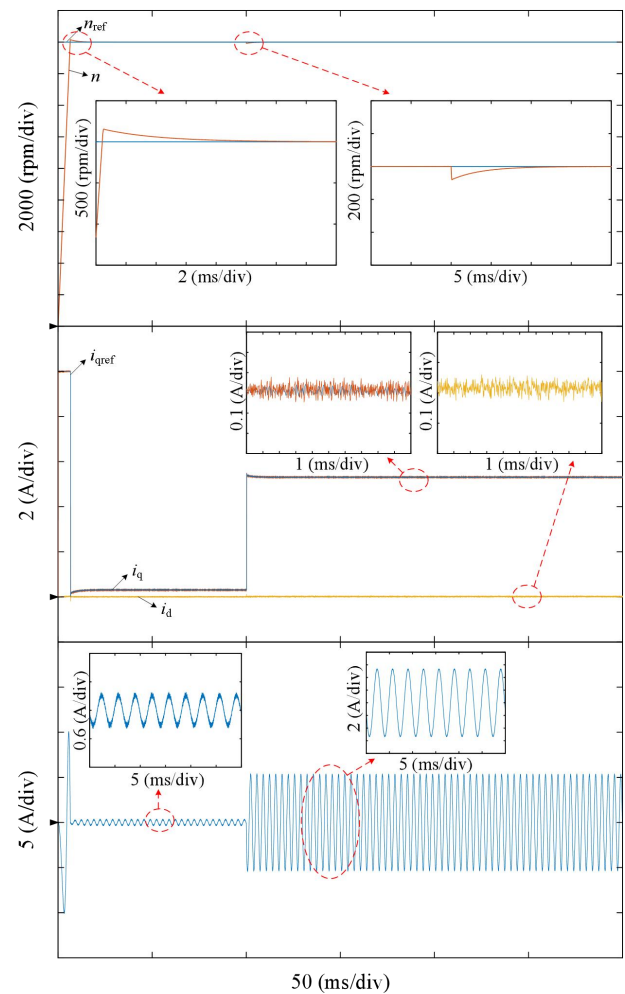


Fig. 7. Simulation Results under Parallel-connection Dual-loop Two-time-scale Control: (a) Speed Dynamic, (b) Currents Performance, (c) Phase Current Waveforms.

scale control is better. The specific comparison data are listed in Table II. Overshoots δ of the speed control under PI and two-time-scale control schemes are 1.67% and 0.83%, with peak times t_p of 6.71 ms and 6.51 ms, respectively. This finding indicates that the proposed method in this study achieves faster states responses than the PI control scheme. In addition, the setting time of the two-time-scale control is 8.5 ms, which is shorter than the PI control's setting time of 11.2 ms. The sudden load of 0.003 N·m torque is placed on the motor system at 0.1 s, and this leads to speed reductions of 0.88% and 0.44% under PI control and two-time-scale control, respectively. All performance indexes of the speed loop under the two control strategies demonstrate that the dynamic property via parallel-connection dual-loop two-time-scale control shows evident advantages over that of the series-connection dual-loop PI control.

The steady-state current ripple values of the two-time-scale control and PI control for the current loop are 0.08 A and 0.1 A, respectively. This finding indicates the enhanced static control performance of the proposed control scheme. Therefore, the proposed control scheme can successfully provide better dynamic and static control performances of HSPMSMs according to the figures and data comparisons.

TABLE II
PERFORMANCE COMPARISON

Index		PI Control	Two-time-scale Control
Speed Loop	Overshoot δ (%)	1.67	0.83
	Peak Time t_p (ms)	6.71	6.51
	Setting Time t_s (ms) ($\Delta=0.5\%$)	11.2	8.50
	Sudden Loading Speed Decreases (%)	0.88	0.44
Current Loop	Steady State Current Ripple (A)	0.10	0.08

V. CONCLUSIONS

A parallel-connection dual-loop two-time-scale control strategy is put forward for HSPMSMs in this study. In this method, the HSPMSMs model rearranged in singular perturbation form is decoupled into slow and fast subsystems. An H_∞ control algorithm for slow subsystem with consideration of disturbance is designed on the basis of linear varying parameter technique. The sliding mode control

scheme is synthesized for fast subsystem with consideration of disturbance. And stabilities of the two subsystems are proven separately. A composite controller is obtained by combining these two subcontrollers. This control strategy is validated via a simulation experiment. And the control performances of the proposed method are compared with the control results of series-connection dual-loop PI method. The comparison results show that the system under the two-time-scale control strategy presents better dynamic and static performances.

REFERENCES

- [1] A. Boglietti, A. Cavagnino, A. Tenconi and S. Vaschetto. "Key Design Aspects of Electrical Machines for High-Speed Spindle Applications," *Proceedings of the 36th Annual Conference on IEEE Industrial Electronics Society*, 2010, pp. 1735–1740.
- [2] M. S. Lim, J. M. Kim, Y. S. Hwang and J. P. Hong. "Design of an Ultra-High-Speed Permanent-Magnet Motor for an Electric Turbocharger Considering Speed Response Characteristics," *IEEE/ASME Transactions on Mechatronics*, vol. 22, no. 2, pp. 774–784, 2017.
- [3] D. H. Jung, J. K. Lee, J. Y. Kim, I. S. Jang, J. Lee and H. J. Lee. "Design Method of an Ultra-High Speed PM Motor/Generator for Electric-Turbo Compounding System," *IEEE Transactions on Applied Superconductivity*, vol. 28, no. 3, pp. 1–4, 2018.
- [4] C. L. Lin, H. Y. Jan and N. C. Shieh. "GA-based multiobjective PID control for a linear brushless DC motor," *IEEE/ASME Transactions on Mechatronics*, vol. 8, no. 1, pp. 56–65, 2003.
- [5] Y. Li, Y. Zhou, C. Zhao and Y. Qin. "Dead-beat control of permanent magnet synchronous motor based on extended voltage vectors set," *Energy Reports*, vol. 6, pp. 1377–1382, 2020.
- [6] Y. Zhang and H. Yang. "Model Predictive Torque Control of Induction Motor Drives With Optimal Duty Cycle Control," *IEEE Transactions on Power Electronics*, vol. 29, no. 12, pp. 6593–6603, 2014.
- [7] J. Xu, B. Zhang, H. Fang and H. Guo. "Guaranteeing the fault transient performance of aerospace multiphase permanent magnet motor system: An adaptive robust speed control approach," *CES Transactions on Electrical Machines and Systems*, vol. 4, no. 2, pp. 114–122, 2020.
- [8] H. Melkote, F. Khorrami, S. Jain and M. S. Mattice. "Robust adaptive control of variable reluctance stepper motors," *IEEE Transactions on Control Systems Technology*, vol. 7, no. 2, pp. 212–221, 1999.
- [9] M. Preindl and S. Bolognani. "Model Predictive Direct Speed Control with Finite Control Set of PMSM Drive Systems," *IEEE Transactions on Power Electron.*, vol. 28, no. 2, pp. 1007–1015, 2013.
- [10] W. Tu, G. Luo, Z. Chen, C. Liu and L. Cui. "FPGA Implementation of Predictive Cascaded Speed and Current Control of PMSM Drives With Two-Time-Scale Optimization," *IEEE Transactions on Industrial Informatics*, vol. 15, no. 9, pp. 5276–5288, 2019.
- [11] Y. Zhang, Z. Yang, W. Duan, X. Hu, Y. Wang, and Z. Yu. "Absolute Stability Criteria of Singularly Perturbed Lur'e Systems with Time-Varying Delays," *Engineering Letters*, vol. 30, no. 1, pp. 369–374, 2022.
- [12] B. Salgadobizzo, G. A. Pimentel, R. Castro, and R. Perez-Ibacache. "Model reduction and feedback design based on singular perturbation method applied to a lumped der-microgrid model," *International Journal of Electrical Power & Energy Systems*, vol. 132, no. 2, pp. 1–10, 2021.
- [13] Y. Wang, P. Shi and H. Yan. "Reliable Control of Fuzzy Singularly Perturbed Systems and Its Application to Electronic Circuits," *IEEE Transactions on Circuits and Systems I: Regular Papers*, vol. 65, no. 10, pp. 3519–3528, 2018.
- [14] Y. Yuan, S. Fuchun, L. Huaping and W. Qinyi. "Multi-objective robust control of flexible-link manipulators based on fuzzy singularly perturbed model with multiple perturbation parameters," *Proceedings of the 31st Chinese Control Conference*, 2012, pp. 2613–2617.
- [15] X. Xu, R. M. Mathur, J. Jiang, G. J. Rogers and P. Kundur. "Modeling effects of system frequency variations in induction motor dynamics using singular perturbations," *IEEE Transactions on Power Systems*, vol. 2, no. 2, pp. 764–770, 2000.
- [16] W. Kim, D. Shin, Y. Lee, and C. C. Chung. "Simplified torque modulated microstepping for position control of permanent magnet stepper motors," *Mechatronics*, pp. 162–172, 2016.
- [17] V. Vasquez-Lopez, R. Castro-Linares and Ja. Alvarez-Gallegos. "Reduced order controller of two-time-scale discrete non-linear systems: application to the regulation of a pm stepper motor," *American Control Conference*, 2002, pp. 1837–1842.
- [18] H. Hofmann, and S. R. Sanders. "Speed-sensorless vector torque control of induction machines using a two-time-scale approach," *IEEE Transactions on Industry Applications*, vol. 34, no. 1, pp. 169–177, 1998.
- [19] P. Kokotovic, H. K. Khalil and J. O'Reilly. *Singular perturbation methods in control analysis and design*. Academic Press, London, 1986.
- [20] K. Zhou. *Robust Optimal Control: Theories and Applications*. National Defense Industry Press, Beijing, 2002.
- [21] Y. Zhang, Z. Liu, Z. Yang, and H. Si. "Robust Control of Wind Turbines by Using Singular Perturbation Method and Linear Parameter Varying Model," *Journal of Control Science and Engineering*, no. 3, pp. 1–10, 2016.
- [22] F. D. Bianchi, H. D. Battista, and R. J. Mantz. *Wind Turbine Control Systems Principles, Modelling and Gain Scheduling Design*, Springer, London, UK, 2007.

Yan Zhang Dr. Zhang received her bachelor degree in Mathematics in 2010 and PhD degree in Automation in 2015 from Nanjing University of Science and Technology, Nanjing, China. Dr. Zhang had been a visiting scholar at Idaho State University in America during the period of 2013–2014. She is currently a lecturer in School of Intelligent Science and Control Engineering at the Jinling Institute of Technology. She is also working as a postdoctor in the School of Automation Engineering, Nanjing University of Aeronautics and Astronautics. Her research interests include singular perturbation method, model predictive control, optimal control, and high-speed permanent magnet synchronous motor drive system.